

Nuclear Magnetic Resonance Fragment-Based Identification of Novel FKBP12 Inhibitors

John L. Stebbins,^{†,‡} Ziming Zhang,^{†,‡} Jinhua Chen,^{†,‡} Bainan Wu,[†] Aras Emdadi,[§] Megan E. Williams,[§] John Cashman,[△] and Maurizio Pellecchia^{*,†}

Infectious and Inflammatory Disease Center, Cancer Center, Burnham Institute for Medical Research, 10901 North Torrey Pines Road, La Jolla, California 92037, University of California at San Diego, Division of Biological Sciences, 9500 Gilman Drive, La Jolla, California 92093, and Human BioMolecular Research Institute, 5310 Eastgate Mall, San Diego, California 92121

Received June 25, 2007

Peptidyl–prolyl *cis–trans* isomerases are a group of cytosolic enzymes initially characterized by their ability to catalyze the *cis–trans* isomerization of peptidyl–prolyl bonds. This represents a significant event for protein folding because *cis*-proline introduces critical bends within the protein conformation. FK506-binding proteins (FKBPs) represent one of the three families of enzymes sharing peptidyl–prolyl *cis–trans* isomerase activity. Inhibitors of FKBP12, in particular, have potent neurotrophic properties both in vivo and in vitro. Here, we describe a fragment-based unbiased nuclear magnetic resonance drug discovery approach for the identification of novel classes of chemical inhibitors against FKBP12. Compared to FK506, the fragment-based FKBP12 inhibitors developed herein possess significant advantages as drug candidates.

Introduction

Peptidyl–prolyl *cis–trans* isomerases (PPIs⁴) are a group of cytosolic enzymes initially characterized by their ability to catalyze the *cis–trans* isomerization of peptidyl–prolyl bonds.¹ This represents a significant event for protein folding because *cis*-prolines introduce essential bends within protein conformations. FK506-binding proteins (FKBPs) are one of three families of enzymes sharing PPI activity. FKBPs are found in all classes of organisms, some highly conserved while others are unique.² These proteins have multiple cellular roles, the best known being as receptors for medically important immuno-suppressors such as FK506. However, most cellular FKBP functions are still unknown. FKBP12 represents the minimal peptide sequence that harbors the two hallmark properties of FKBPs: PPI activity and immunophilin FK506 binding.

Inhibitors of the prolyl isomerase activity of FKBP12 possess potent neurotrophic properties in vivo and in vitro,^{3–6} a function that may be distinct from its immunosuppressive activity. This finding makes them obvious therapeutic candidates for a variety of neurodegenerative diseases such as Parkinson's disease, Alzheimer's disease, amyotrophic lateral sclerosis, diabetic neuropathy, nerve injury, cerebral ischemia, and traumatic brain injury. As a result, research in both industry and academia aimed at the development of novel FKBP12 inhibitors has been initiated. However, the small molecule inhibitors of FKBP12 developed thus far are invariably based on the natural immunophilin FK506.^{3,7–21} Here we describe a fragment-based unbiased nuclear magnetic resonance (NMR) drug discovery

approach^{22,23} for the identification of novel classes of chemical inhibitors against FKBP12.

Results and Discussion

The relatively small size of FKBP12 (10 kDa) makes it amenable to protein-NMR spectroscopy techniques, such as two-dimensional (2D) [¹⁵N, ¹H] or 2D [¹³C, ¹H] experiments, designed for the detection of ligand binding. These approaches are preferential to transfer ligand-based techniques as they provide intrinsic structural binding site information and are largely void of false positives or false negatives.^{23,24} However, the use of 2D [¹⁵N, ¹H]²⁵ or 2D [¹³C, ¹H] correlation spectra^{26,27} as a screening method requires relatively large amounts of protein per sample (> 100 μM) and relatively lengthy measurement times. To ameliorate these problems we propose a primary screen employing simple one-dimensional (1D) ¹H NMR experiments, acquired in the presence and absence of a mixture of potential ligands. Eventual resonance overlap with resonance lines of test compounds is resolved by using ¹³C-labeled samples and 1D ¹³C-edited ¹H NMR experiments. This protocol has the intrinsic advantage of requiring relatively small protein concentrations (10–50 μM) and relatively short measurement times (typically from 15 min to 1 h depending on the spectrometer used and the protein's molecular weight). Because of the ¹³C filter, signals arising from the test ligands or from solvent and buffers are effectively suppressed, thereby enabling the screening of compounds in mixtures without protein spectrum interference. Another advantage of this technique is that observables can also be detected in the aliphatic region of the protein spectrum (1 ppm and below), a region rarely populated by signals from organic molecules. In such cases, the use of ¹³C labeling would not be necessary. This is illustrated in Figure 1 where the aliphatic region of the 1D ¹H NMR spectrum of FKBP12 is shown in the absence and presence of compound **1** (BI-12B10). The protein spectrum of the aliphatic region is generally not affected by DMSO (up to 5%) or small changes in buffer conditions, making identification of potential ligands straightforward and unambiguous. In addition, initial potency ranking can be obtained by direct 1D ¹H NMR chemical shift titrations. An approximate *K_D* value of 3 μM was obtained for **1** (Figure 1), which compares well with the reported *K_D* value of 2 μM.²⁵

* To whom correspondence should be addressed. Tel.: 858-646-3159. Fax: 858-713-9925. E-mail: mpellecchia@burnham.org.

[†] Burnham Institute for Medical Research.

[‡] These authors contributed equally to this work.

[§] University of California at San Diego.

[△] Human BioMolecular Research Institute.

⁴ Abbreviations: PPI, peptidyl–prolyl *cis–trans* isomerase; FKBP, FK506-binding protein; NMR, nuclear magnetic resonance; HSQC, heteronuclear single quantum correlation; DMAP, dimethylaminopyridine; DMSO, dimethylsulfoxide; DMF, dimethylformamide; EDC, *N*-ethyl-*N'*-(3-dimethylaminopropyl)-carbodiimide hydrochloride; HOBt, 1-hydroxy-1*H*-benzotriazole hydrate; MeOH, methanol; LiOH, lithium hydroxide; NaOH, sodium hydroxide; NEt₃, triethylamine; THF, tetrahydrofuran; rt, room temperature.

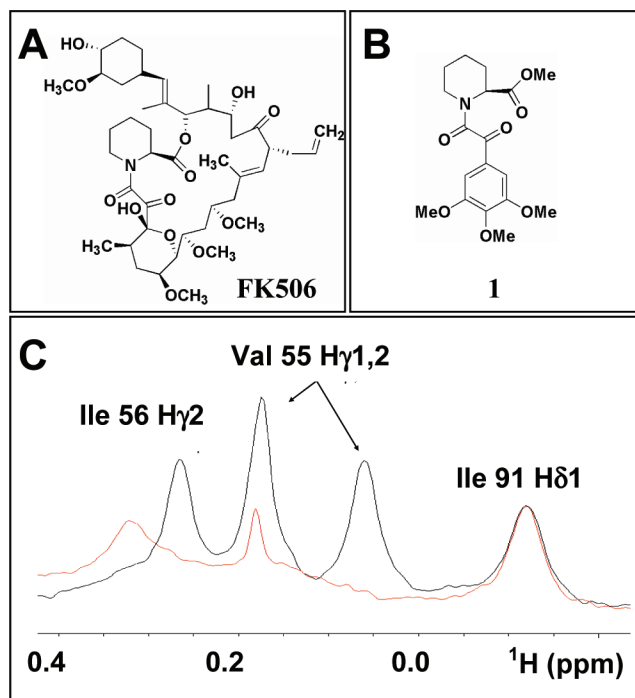


Figure 1. Chemical structure of (A) FK506 and (B) **1**. (C) 1D ^1H aliphatic NMR-based ligand screening. ^1H NMR spectra of the FKBP12 aliphatic region measured at 27 °C in the presence (red) and in the absence (black) of **1**.

Table 1. Statistics of the Assembled Library for the Proposed Fragment-Based Screening^a

database	number of compounds	diversity (%)
MayBridge	491	79
Life Chemicals	485	95
ChemBridge (I)	1010	82
ChemBridge (II)	976	89
Overall	2962	82
Natural Product	602	49

^a The structures have been deposited in PubChem (<http://pubchem.ncbi.nlm.nih.gov>). The diversity was computed using UNITY, as implemented in SYBYL, version 7.0 (TRIPOS Inc., St. Louis, MO).

Fragment-Based Drug Discovery. As is typical of fragment-based drug discovery, we assembled a scaffold library composed of ~3000 fragments (Table 1). Given the ability of the described NMR-based screening technique to detect even weak binding events, with affinities in the micromolar to millimolar range, such a library of representative compounds should suffice to identify preferential structures. Hits would subsequently be used as starting points for iterative optimizations, using several different strategies, the simplest being selecting compound analogues. The selection of a sublibrary is also necessary to overcome the intrinsic low throughput of NMR-based strategies versus traditional biochemical assays. The scaffold library used in this study was assembled from three different sources (Table 1), and the chemical structures of the library components have been deposited into PubChem (<http://pubchem.ncbi.nlm.nih.gov>). In addition, the library also includes a collection of 602 natural products (MicroSource) amenable to NMR screening.

The ability of library components to interact with FKBP12 was determined by 1D aliphatic- ^1H NMR measurements using a 32 μM protein sample and mixtures of 10 compounds per sample (125 μM each). Compound mixtures producing significant chemical shift variations (e.g., larger than 0.08 ppm) were subsequently deconvoluted. Ultimately, by employing this strategy, we identified the classes of novel FKBP12 ligands

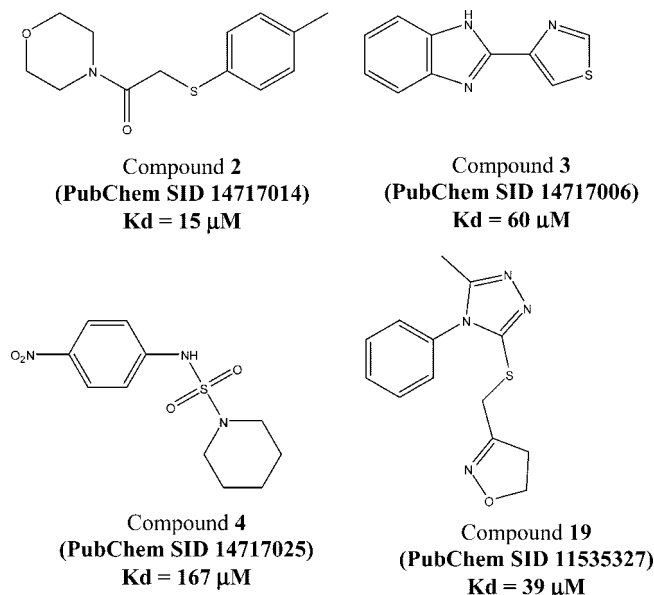


Figure 2. Chemical structures and estimated binding affinities of hit compounds from the NMR screen.

shown in Figure 2. As an example, we report in Figure 3 data relevant to compound **2** (PubChem ID number 14717014). This compound induces chemical shift changes upon binding in the aliphatic region of the spectrum similar to those observed with **1**.²⁵ Compounds **3** (14717006) and **4** (14717025) resemble previously identified FKBP12 inhibitors, which provides a further validation of this approach. Compound **2**, while also displaying similarities to **1** and other FK506-derived inhibitors, presents novel structural features that could not have been easily anticipated by simply modifying these compounds. For example, the previously identified FK506-derived inhibitors require the presence of an α -keto amido group (Figure 1), a moiety that is critical for the ability of these compounds to bind FKBP12. Attempts to replace the α -keto amido group with more stable functional groups have been recently reported.^{17,29} As **2** lacks this undesired functionality, it represents a more promising starting point for the development of novel FKBP12 inhibitors.

Structure–Activity Relationships. Initial structure–activity relationship data were obtained by selecting and testing 51 commercially available derivatives of **2** (Table 2), 12 derivatives of **3** (Supporting Information, Table 1) and 13 derivatives of compound **4** (Supporting Information, Table 2). Compound dissociation constants for FKBP12 were determined by 1D-aliphatic ^1H NMR and isothermal titration calorimetry (ITC; Figure 3).

Based on the SAR data obtained with **2** (Table 2) and its similarity with **1**, the following chemical modifications were made: the synthesis of bidentate compounds derivatizing the morpholino group with secondary site binders and the modification of the linker region between the phenyl ring and the morpholino groups. In addition, SAR data relative to the phenyl ring of **2** suggests that a bulkier, hydrophobic group such as an isopropyl in the *para* position may be preferred (Schemes 1–4). These strategies lead to the identification of submicromolar binders for FKBP12 (Table 3).

Mapping Studies. To further characterize the binding affinities of the novel compounds for FKBP12, we collected and overlaid 2D [^{15}N , ^1H] spectra of FKBP12 in presence of various compounds. Among the five compounds tested, compound **6** (BI-69A8) and compound **10** (BI-69A5) resulted in significant cross-peak movements, such as G51 and Y26, under the same

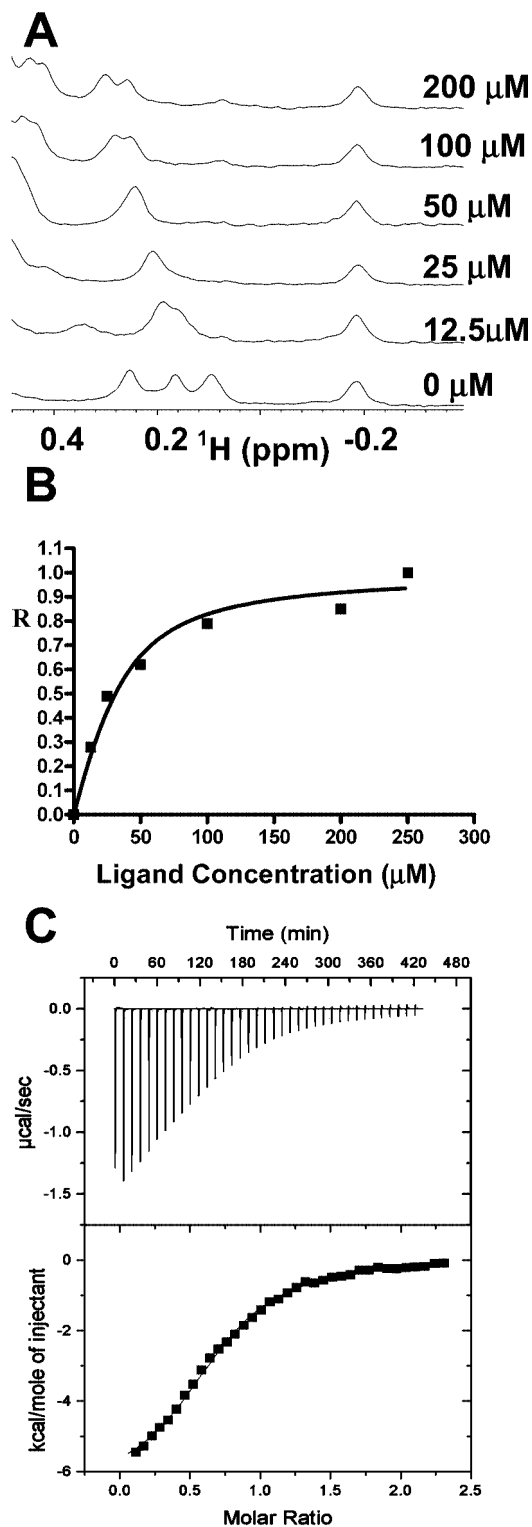


Figure 3. Binding data relative to **2**. (A) 1D ^1H aliphatic NMR spectra of $32\ \mu\text{M}$ FKBP12 in the presence of different concentrations of ligand. (B) Fractional changes (R) of chemical shifts in FKBP12 as a function of ligand concentration. The experimental data were fitted to the nonlinear equation as described in the methods. $K_D = 15.0\ \mu\text{M}$. (C) ITC data: The top panel shows the heat signals for ligand injections into a sample cell containing FKBP12 ($100\ \mu\text{M}$). The bottom panel shows the integrated heat of each injection after correcting for the heat of dilution of the ligand. The curve represents the best fit to a model involving a single set of independent sites. $K_D = 9.4\ \mu\text{M}$, which is in close agreement with the NMR titration value reported above.

molar ratio (Figure 4). In agreement with 1D chemical shift titration, 2D mapping suggests that **6** and **10** have the strongest

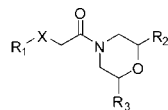
binding affinities (Table 3). Mapping chemical shift perturbations (Figure 4) on the three-dimensional (3D) structure of FKBP12 upon binding identifies the binding pocket for **6**. Similar chemical shift mapping data for compounds reported in Table 3 were also obtained (not shown). The nature of the chemical shifts of the compounds classes listed in Figure 2 clearly indicates that compounds occupy different subpockets within the binding domain of the enzyme. In agreement with this observation, a displacement assay based on NMR chemical shift mapping shows that while **2** and **3** occupy different subpockets their simultaneous presence is not tolerated (data not shown).

Furthermore, we performed molecular docking studies by using the X-ray coordinates of FKBP12 in complex with a previously derived FK506 mimic compound.¹⁷ From these models and in agreement with NMR chemical shift mapping data, the morpholino group adopts a binding mode that is similar to the piperidine of the previously reported compounds (such as **1**), while the sulfur atom and the *p*-isopropyl group extend to occupy a smaller hydrophobic pocket at the edge of the binding site (Figure 5). However, because of the insertion of the oxygen atom, the morpholino moiety is shifted with respect to the corresponding piperidines in the previously reported compounds. As a result, the carbonyl of the amide group of **6** is involved in the crucial hydrogen bonding interaction with the hydroxyl group of Tyr 26 (Figure 5).¹⁷ In FK506 and related compounds, this hydrogen bonding was previously recognized as being essential for the binding affinity and was attributed to the α -keto group.^{3,16–21} Only recently, attempts to replace this α -keto group were made with a fluorinated compound derivative (Figure 5D). In agreement with this model, corresponding substitutions of the morpholino group with previously reported second site binders such as a pyridine ring (Table 3) resulted in less active compounds, presumably due to the different conformational arrangement of the aliphatic ring in the molecule. Similarly, as one would predict by the model (Figure 5), replacing the methylene group in **6** with a $-\text{CF}_2-$ group does not result in increased activity (Table 3).

Therefore, we have obtained a molecular model that can explain both experimental NMR chemical mapping studies and observed SAR related to this series of compounds. We anticipate that this model could be very useful in formulating hypotheses for further derivatizations of **6** and related compounds.

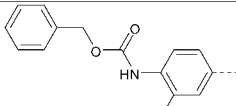
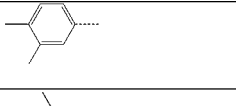
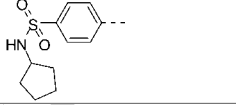
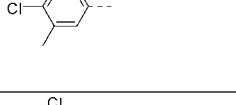
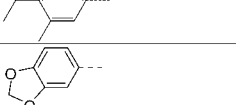
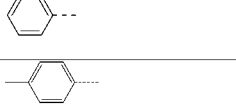
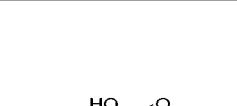
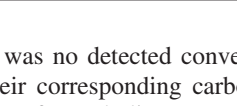
Cell-Based Evaluation. To test the hypothesis that the purported FKBP12 binders would stimulate neurite outgrowth similar to that seen with FK506, we treated primary cortical neurons with either $0.1\ \mu\text{M}$ or $1\ \mu\text{M}$ of test compound for 72 h and then calculated average neurite length. As expected, FK506 treatment resulted in an increase in average neurite length (Figure 6). Treatment with several of the compounds identified in this study resulted in stimulation of neurite outgrowth. In comparison to control treatment, most compounds resulted in robust neurite outgrowth, an example of which can be seen in Figure 6. In most cases, neurite outgrowth was stimulated to a level comparable to that seen with FK506 (Figure 6). In agreement with binding affinity determinations (Figure 2), **3** demonstrated the weakest effect, while **6** (Table 3) was the most potent. Thus, we feel that these compounds have biological activity similar to FK506 in this assay.

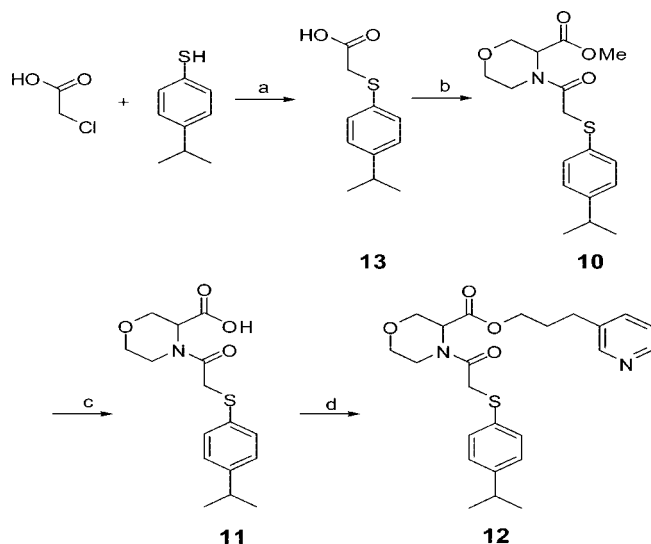
While these data strongly suggest FKBP12 is the relevant target of the compounds, we cannot rule out the possibility that the molecules could interact with other closely related targets (e.g., FKBP12.6, FKBP13, FKBP25, FKBP38, and FKBP38).²⁸ However, when tested against Pin1, another proline *cis-trans*

Table 2. Structure–Activity Relationships Data Relative to Derivatives of **2**

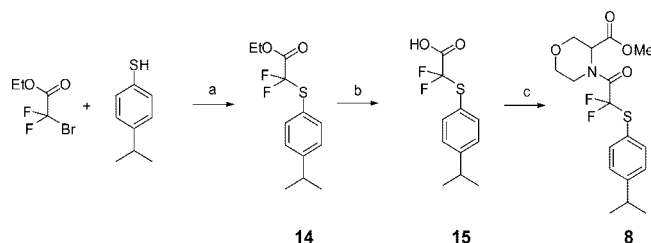
COMPOUND (PubChem Substance ID)	X	R1	R2	R3	KD (μM)	Compound	X	R1	R2	R3	KD (μM)
Compound 20 (14717010)	S		II	II	>1400	Compound 44 (14717085)	O		H	H	100
Compound 21 (14717011)	S		H	H	>1400	Compound 45 (14717086)	O		H	H	>2400
Compound 22 (14717036)	S		H	H	>1400	Compound 46 (14717088)	O		H	H	357
Compound 23 (14717013)	S		II	II	ITC:23.5 NMR:15.3	Compound 47 (14717089)	O		H	H	576
2	S		H	H	ITC:9.4 NMR:15	Compound 48 (14717091)	O		H	H	>1000
Compound 24 (14717015)	S		II	II	ITC:19 NMR:15	Compound 49 (14717092)	O		H	H	>5000
Compound 25 (14717053)	S		H	H	>3700	Compound 50 (14717093)	O		H	H	>1500
Compound 26 (14717023)	S		H	H	453	Compound 51 (14717094)	O		II	II	>1000
Compound 27 (14717022)	S		CH ₃	CH ₃	726	Compound 52 (14717095)	O		II	II	576
Compound 28 (14717038)	S		CH ₃	CH ₃	>4000	Compound 53 (14717096)	O		H	H	576
Compound 29 (14717068)	O		H	H	>1029	Compound 54 (14717097)	O		H	H	>1000
Compound 30 (14717069)	O		II	II	>1029	Compound 55 (14717100)	O		H	H	>5000
Compound 31 (14717070)	O		H	H	357	Compound 56 (14717103)	O		II	II	>2500
Compound 32 (14717071)	O		H	H	450	Compound 57 (14717104)	O		II	II	>5000
Compound 33 (14717072)	O		H	H	>1500	Compound 58 (14717105)	O		H	H	576
Compound 34 (14717073)	O		H	H	>2500	Compound 59 (14717106)	O		H	H	576
Compound 36 (14717077)	O		H	H	>1000	Compound 60 (14717107)	O		H	H	>5000
Compound 37 (14717078)	O		H	H	>1000	Compound 61 (14717108)	O		H	H	755
Compound 38 (14717079)	O		II	II	755	Compound 62 (14717109)	O		H	H	>2500
Compound 39 (14717080)	O		H	H	231						
Compound 40 (14717081)	O		H	H	755						
Compound 41 (14717082)	O		II	II	>1500						
Compound 42 (14717083)	O		H	H	123						
Compound 43 (14717084)	O		H	H	231						

Table 2. Continued

Compound 63 (14717110)	O		H	H	>1500	Compound 67 (14717098)	O		CH ₃	CH ₃	>5000
Compound 64 (14717112)	O		H	H	755	Compound 68 (14717099)	O		CH ₃	CH ₃	>5000
Compound 65 (14717111)	O		H	H	187	Compound 69 (14717101)	O		CH ₃	CH ₃	>5000
Compound 66 (14717113)	O		H	H	576	Compound 70 (14717035)	SO ₂		H	H	>5000

Scheme 1^a

^a Reagents and conditions: (a) NaOH, H₂O, 80 °C, 2 h, then HCl; (b) EDC, HOBT, NEt₃, methyl morpholine-3-carboxylate, DMF, rt, 12 h; (c) LiOH, THF/H₂O, rt, 5 h, then HCl; (d) EDC, DMAP, 3-(pyridin-3-yl)propan-1-ol, DMF, rt, 12 h.

Scheme 2^a

^a Reagents and conditions: (a) Na₂CO₃, DMF, 60 °C; (b) LiOH, THF/H₂O; (c) EDC, HOBT, NEt₃, methyl morpholine-3-carboxylate, DMF, rt, 12 h.

isomerase,^{30,31} the compounds did not show any appreciable binding (data not shown). Therefore, our compounds may prove to be molecular probes useful in the elucidation of the roles of FKBP12 related proteins in cell.

Metabolic Stability Studies. Compounds 8 (BI-69B7), 9 (BI-12B8), 1, 10, 11 (BI-69A6), 12 (BI-69A7), and 6 (Table 3), as well as FK506, were assayed for their metabolic stability in the presence of pooled human liver microsomes and an NADPH generating system. With the exception of 11 and FK506, which showed half-lives of greater than 60 min, the compounds exhibited half-lives of about 40 min. On the basis of RP-HPLC

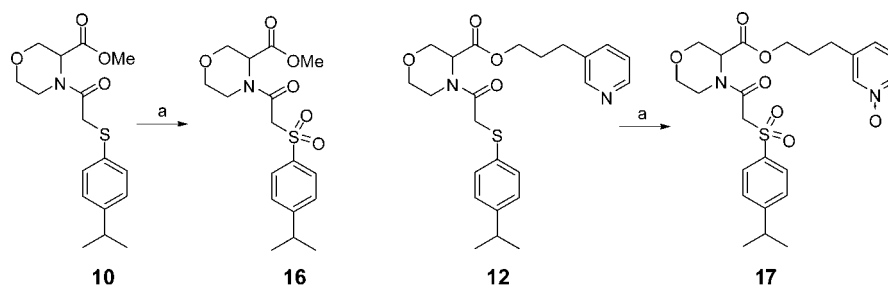
analysis, there was no detected conversion of esters 8, 1, 10, and 12 into their corresponding carboxylic acids, suggesting the major route of metabolism was not ester hydrolysis. To investigate the apparent metabolic stability of this series of compounds, their ability to inhibit the conversion of testosterone to 6-hydroxy testosterone by human liver microsomes at concentrations of 10 μM was examined. At 10 μM, 12 and FK506 completely inhibited the formation of 6-hydroxy testosterone. The other compounds examined showed estimated IC₅₀ values of approximately 10 μM. Detailed determination of the IC₅₀ of 12 and FK506 for inhibition of testosterone hydroxylase showed they possessed IC₅₀ values of 0.81 μM and 2.26 μM, respectively. It is likely that the pyridine moiety of 12 and the vinyl group of FK506, respectively, are responsible for the potent testosterone 6-hydroxylase inhibition activity. Regardless, the fragment-based approach has successfully resulted in the elaboration of smaller molecular weight compounds devoid of the metabolic inhibitory activity of FK506. Development of drug-like materials without the potential for adverse drug–drug interactions may hold promise for a new class of neuroprotective agents.

In conclusion, our fragment-based data clearly demonstrate the effectiveness and usefulness of our approaches in the rapid identification and optimization of novel molecular tools. We feel that this method will be useful for further lead development and optimization of therapeutic candidates for a variety of neurodegenerative diseases.

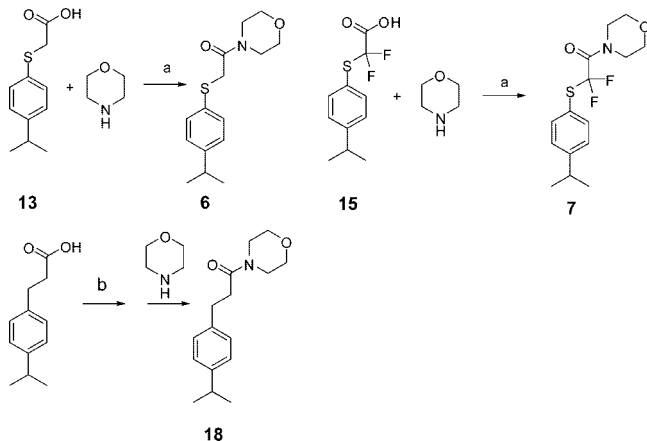
Material and Methods

Protein Expression and Purification. The gene coding for the human FKBP12 was amplified with PCR and subcloned into pET21a using the NdeI and XhoI cloning sites. The resulting proteins contain eight extra C-terminal amino acid residues (LEHHHHHH). The protein was expressed in the *Escherichia coli* strain BL21(DE3) and purified using Ni²⁺ affinity chromatography. The uniformly ¹⁵N-labeled FKBP12 was produced by growing the bacteria in M9 minimal media containing ¹⁵NH₄Cl as the sole nitrogen source. The NMR samples were dissolved in 20 μM sodium phosphate buffer (pH 7.5) containing 90%/10% (H₂O/²H₂O) or 99.5% ²H₂O.

NMR Spectroscopy. Spectra were acquired on a 600 MHz Bruker Avance spectrometer equipped with TXI probe and z-shielded gradient coils or on a 600 MHz Bruker Avance equipped with TCI cryoprobe. Ligand binding was detected at 27 °C by comparing the aliphatic region of 1D ¹H spectra of 32 μM FKBP12 in the presence and in the absence of 125 μM compounds. Compounds were initially tested at mixtures of 10, and then individual compound mixtures that caused significant perturbations in the spectrum (>0.08 ppm) were characterized further.

Scheme 3^a

^a Reagents and conditions: (a) *m*CPBA, CH₂Cl₂, rt, 72 h.

Scheme 4^a

^a Reagents and conditions: (a) EDC, HOBt, DMF; (b) (COCl)₂, DMF (cat), CH₂Cl₂.

Dissociation equilibrium constants (K_D) of ligands were determined by monitoring the protein chemical shift changes as a function of ligand concentration. Data were collected for a set of resolved FKBP12 ¹H NMR resonances and fitted to a single binding site model according to the following equation:²⁵ $R = (\delta_{\text{obs}} - \delta_f) / \Delta_{\text{b-f}}$, where R is the mole fraction of the protein–ligand complex used for the K_D calculation, δ_{obs} is the observed chemical shift for NMR titrations, δ_f is the chemical shift of the free protein, and $\Delta_{\text{b-f}}$ is the difference in chemical shift between the free and the fully complexed protein.

All NMR data were processed and analyzed using TOPSPIN2.0 (Bruker BioSpin Corp., Billerica, MA) and SPARKY.³² For chemical shift mapping, the NMR samples contained 0.1 mM ¹⁵N-labeled FKBP12, 100 mM potassium phosphate buffer (pH 6.5), 5% DMSO, and 5% D₂O. 2D [¹⁵N, ¹H]-HSQC experiments were acquired using 32 scans with 2048 and 128 complex data points in the ¹H and ¹⁵N dimensions at 300 K.

Binding Constant Determination by Isothermal Titration Calorimetry. Isothermal titration calorimetry (ITC) was performed on a VP-ITC calorimeter from Microcal (Northampton, MA). A total of 8 μ L of ligand solution (1.0 mM) were injected into the cell containing 100 μ M FKBP12 per injection. In each experiment, 37 injections were made. All titrations were performed at 23 °C in PBS buffer supplemented with 10% DMSO. Experimental data were analyzed using Microcal Origin software provided by the ITC manufacturer (Microcal, Northampton, MA).

Neurite Outgrowth Assay. E18/19 cortical cells from Long-Evans rats were cultured as previously described,³³ with the following minor modifications. The cortex was dissected in ice-cold HBSS (6.5 g/L glucose), digested in 10 U/mL Papain in dissociation media (2 \times 20 min), and dissociated in culture media. The dissociated neurons were plated on polylysine laminin-coated 24-well plates at 3 \times 10⁵ cells per well in glutamine-free Basal Media Eagle (Sigma) supplemented with glutamine (to 1 mM), N2 (to 1%; Gibco), and fetal bovine serum (5%). Cells were allowed

to attach for 48 h, after which various doses of experimental compounds were applied. After a 24 h incubation, cells were transfected with GFP expressing plasmid (pBOS-EGFP) using Lipofectamine 2000, after which various doses of experimental compounds were reapplied. Neurite length of at least 10 neurite containing cells was quantified using Image-Pro Plus (Media Cybernetics, Bethesda, MD).

Immunostaining of Dissociated Cells on Coverslips. Cells were fixed for 15 min at room temperature with 4% paraformaldehyde/0.1% Triton X-100 followed by blocking nonspecific binding for 2 h with 3% BSA and 0.1% Triton X-100 in PBS. Cells were then incubated with primary antibody for 2 h at room temperature in 3% BSA and 0.3% Triton X-100 in PBS and then with secondary antibody at room temperature for 1 h in 3% BSA and 0.3% Triton X-100 in PBS. Primary antibody used was rabbit polyclonal anti-GFP (1:1000, Invitrogen catalog number A11122). Secondary antibody used was goat antirabbit Alexa Flour 488 (1:1000, Invitrogen, catalog number A11034).

Synthesis of Phenylthioacetylmorpholine and Analogs. All commercially available reagents were used without further purification. Column chromatography was performed with silica gel 60 (35–75 Å). ¹H NMR and ¹³C NMR for QC analysis were acquired on a Varian Inova 300 MHz spectrometer. Chemical shifts are reported in ppm from residual solvent peaks (2.50 and 7.26 for DMSO-*d*₆ and CDCl₃ for ¹H NMR, and 49.0 and 77.16 for DMSO-*d*₆ and CDCl₃ for ¹³C NMR, respectively). High resolution ESI-TOF mass spectra were acquired at the Center for Mass Spectrometry, the Scripps Research Institute, La Jolla, CA. Compounds **6**, **7**, **8**, **10**, **12**, **16**, **17**, and **18** were all found to be in excess of 95% pure as established by LC-MS.

2-(4-Isopropylphenylthio) Acetic Acid; Compound 13 (BI-69A4). 4-Isopropylbenzenethiol (762 mg, 5.0 mmol) was dissolved in a NaOH solution (500 mg, 12.5 mmol) in H₂O (1.2 mL). 2-Chloroacetic acid (472.5 mg, 5.0 mmol) was added and the reaction mixture was heated at 80 °C for 2 h under N₂. The reaction mixture was dissolved in H₂O (100 mL) and was adjusted to pH 2.0 with concentrated HCl. It was extracted with EtOAc. The combined organic phase was extracted with Na₂CO₃ solution (10%). The Na₂CO₃ solution was adjusted to pH 2.0 with concentrated HCl and extracted with EtOAc. It was dried over Na₂SO₄ and solvent was removed to give **13** as a white solid without further purification (450 mg, 43%). ¹H NMR (300 MHz, DMSO-*d*₆) δ 7.28–7.18 (m, 4 H), 3.73 (s, 2 H), 2.84 (sept, $J = 6.9$ Hz, 1 H), 1.17 (d, $J = 6.9$ Hz, 6 H). ¹³C NMR (75 MHz, CDCl₃) δ 176.1, 148.6, 131.0, 127.5, 37.3, 33.9, 24.0. HRMS m/z calcd for C₁₁H₁₃O₂S [M – H][–], 209.0642; found, 209.0635.

Methyl 4-(2-(4-Isopropylphenylthio)acetyl)morpholine-3-carboxylate (10). Triethylamine (150 mg, 1.5 mmol), EDC (114.6 mg, 0.60 mmol), and HOBt (91.8 mg, 0.60 mmol) were added to a solution of **13** (105 mg, 0.50 mmol) in DMF (5.0 mL) under N₂. After the reaction mixture was stirred at rt for 30 min, methyl morpholine-3-carboxylate (90.5 mg, 0.50 mmol) was added. After the reaction mixture was stirred at rt for 12 h, DMF was removed under reduced pressure. It was purified by silica gel flash chromatography (EtOAc–hexanes = 1:4) to give **10** as a colorless oil (70 mg, 42%). The product exists in two amide rotamers in about 10:1

Table 3. Synthesized Compounds and Relative Binding Affinities for FKBP12^a

COMPOUND	STRUCTURE	K _d (μ M)	COMPOUND	STRUCTURE	K _d (μ M)
13		>4000	17		1285
10		0.3*	8		190
11		426	9		204
12		5.6	Compound 71 (BI-69B9)		578
6		0.2*	18		2.3
16		505	7		2.8
			1		3.0

^a *Indicates an estimated value, as compounds bind in the intermediate exchange rate, typical of those with submicromolar affinity.

ratio. For the major rotamer: ¹H NMR (300 MHz, CDCl₃) δ 7.44–7.35 (m, 2 H), 7.21–7.14 (m, 2 H), 5.02 (s, 1 H), 4.41 (d, *J* = 12 Hz, 1 H), 3.94–3.79 (m, 2 H), 3.76 (s, 3 H), 3.73 (s, 1 H), 3.64–3.45 (m, 3 H), 3.48–3.36 (m, 1 H), 2.94–2.82 (m, 1 H), 1.26–1.18 (m, 6 H). ¹³C NMR (75 MHz, CDCl₃) δ 169.7, 169.1, 148.5, 131.4, 127.3, 67.7, 66.3, 52.6, 52.5, 43.8, 36.9, 33.8, 23.9. HRMS *m/z* calcd for C₁₇H₂₄NO₄S [M + H]⁺, 338.1426; found, 338.1423.

4-(2-(4-Isopropylphenylthio)acetyl)morpholine-3-carboxylic Acid (11). A solution of **10** (337 mg, 1.0 mmol) in THF (10.0 mL) was mixed with a solution of LiOH (120 mg, 5.0 mmol) in H₂O (10.0 mL). After the mixture was stirred at rt for 5 h, THF was removed under reduced pressure and the solution was washed with ether (3 \times 20 mL). The solution was adjusted to pH 1.0 with concentrated HCl and was extracted with ether. The combined ether solution was dried over Na₂SO₄. The solvent was removed to give **11** without further purification (200 mg, 62%). ¹H NMR (300 MHz, CDCl₃) δ 7.62 (b, 1 H), 7.42–7.36 (m, 2 H), 7.20–7.14 (m, 2 H), 5.04 (d, *J* = 3.3 Hz, 1 H), 4.43 (d, *J* = 11.7 Hz, 1 H), 3.94–3.70 (m, 3 H), 3.70–3.50 (m, 3 H), 3.50–3.34 (m, 1 H), 2.87 (sept, *J* = 6.9 Hz), 1.23 (s, 3 H), 1.21 (s, 3 H). ¹³C NMR (75 MHz, CDCl₃) δ 173.5, 169.7, 148.7, 131.7, 127.3, 67.5, 66.1, 52.4, 43.8, 36.8, 33.7, 23.8. HRMS *m/z* calcd for C₁₆H₂₂NO₄S [M + H]⁺, 324.1264; found, 324.1263.

3-(Pyridine-3-yl) propyl 4-(2-(4-isopropylphenylthio)acetyl)morpholine-3-carboxylate (12). 3-(Pyridin-3-yl)propan-1-ol (56 mg, 0.41 mmol) was added to a solution of **11** (110 mg, 0.34 mmol) in DMF (5.0 mL). EDC (95 mg, 0.51 mmol) and DMAP (20 mg, 0.17 mmol) were then added. After the reaction mixture was stirred

at rt for 12 h, DMF was removed under reduced pressure and the residue was purified by silica gel flash chromatography (EtOAc–hexanes = 1:2–1:1) to give **12** as a white solid (80 mg, 53%). ¹H NMR (300 MHz, CDCl₃) δ 8.46–8.42 (m, 2 H), 7.50–7.45 (m, 1 H), 7.42–7.34 (m, 2 H), 7.23–7.19 (m, 1 H), 7.19–7.13 (m, 2 H), 5.00 (d, *J* = 3.6 Hz, 1 H), 4.44–4.34 (m, 1 H), 4.25–4.16 (m, 2 H), 3.94–3.82 (m, 1 H), 3.78–3.42 (m, 1 H), 3.70–3.54 (m, 3 H), 3.48–3.38 (m, 1 H), 2.86 (sept, *J* = 6.9 Hz, 1 H), 2.67 (t, *J* = 7.2 Hz, 2 H), 2.04–1.92 (m, 2 H), 2.21 (d, *J* = 6.9 Hz, 6 H). ¹³C NMR (75 MHz, CDCl₃) δ 169.3, 150.0, 147.7, 136.0, 131.4, 127.4, 123.5, 67.9, 66.4, 64.7, 52.7, 43.9, 37.0, 33.8, 30.0, 29.3, 24.0. HRMS *m/z* calcd for C₂₄H₃₁N₂O₄S [M + H]⁺, 443.1999; found, 443.2007.

Ethyl 2,2-Difluoro-2-(4-isopropylphenylthio)acetate; Compound 14 (JCIH150). Ethyl 2-bromo-2,2-difluoroacetate (1.0 g, 5.0 mmol), 4-isopropylbenzethiol (0.75 g, 5.0 mmol), and sodium carbonate (0.53 g, 5.0 mmol) were mixed in DMF (10.0 mL) and heated to 60 °C under N₂ for 12 h. DMF was removed and the residue was purified by silica gel flash chromatography (EtOAc–hexanes = 1:9) to give **14** as a colorless oil (0.70 g, 51%). ¹H NMR (300 MHz, DMSO-*d*₆) δ 7.53 (d, *J* = 8.4 Hz, 2 H), 7.37 (d, *J* = 8.1 Hz, 2 H), 4.32 (q, 2 H), 2.94 (sept, *J* = 6.9 Hz, 1 H), 1.20 (d, *J* = 6.9 Hz, 6 H), 1.14 (t, *J* = 7.2 Hz, 3 H). ¹³C NMR (75 MHz, DMSO-*d*₆) δ 161.2, 160.8, 160.4, 151.9, 136.6, 127.8, 123.8, 120.4, 120.0, 116.2, 63.9, 33.2, 23.5, 13.5. HRMS *m/z* calcd for C₁₃H₁₆F₂O₂SNa [M + Na]⁺, 297.0731; found, 297.0735.

2,2-Difluoro-2-(4-isopropylphenylthio)acetic Acid; Compound 15 (JCIH151). A solution of ethyl 2,2-difluoro-2-(4-isopropylphenylthio)acetate (440 mg, 1.6 mmol) in THF (5.0 mL) was mixed with a solution of LiOH (115 mg, 4.8 mmol) in H₂O (5.0 mL) and

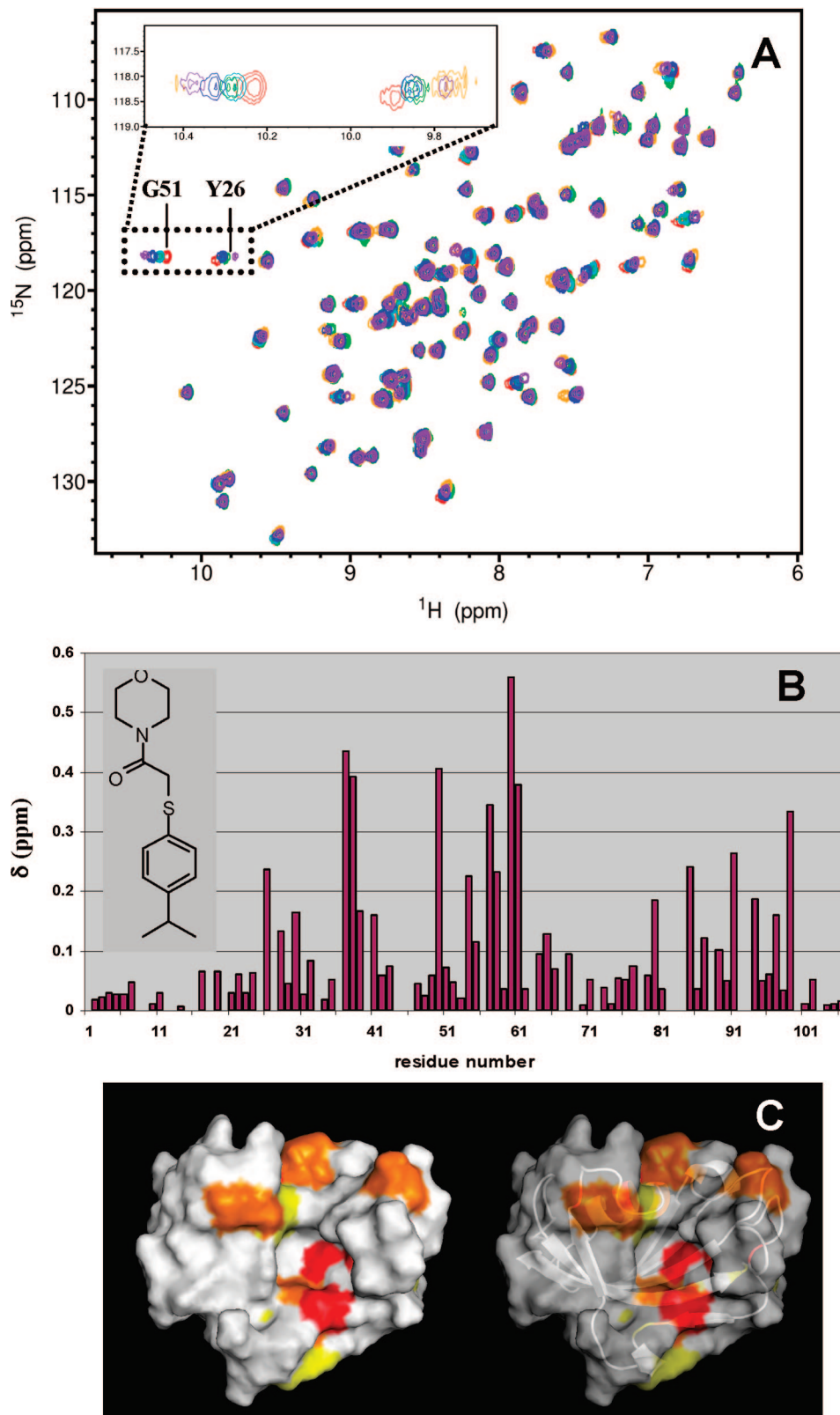


Figure 4. Chemical shift mapping studies. (A) Changes in chemical shifts of FKBP12 ^{15}N -HSQC spectrum upon addition of **6**. The molar ratio of FKBP12 and the compounds are 1:1. (B) Sequential variation of chemical shift changes due to the binding of **6**. Chemical shift changes differences ($\Delta\delta$) between ^{15}N -HSQC spectra of free FKBP12 and **6**-bound FKBP12 were calculated as $\Delta\delta = [(\Delta H_{\text{N}})^2 + (0.17\Delta^{15}\text{N})^2]^{1/2}$. (C) Mapping on a 3D surface representation of the calculated chemical shift changes between free and **6**-bound FKBP12. Colors are white ($\Delta\delta < 0.1$), yellow ($0.1 < \Delta\delta < 0.2$), orange ($0.2 < \Delta\delta < 0.4$), and red ($0.4 < \Delta\delta < 0.6$).

stirred at rt for 2 h. THF was removed under reduced pressure and the solution was washed with ether (3×10 mL). It was acidified to pH 3.0 and was extracted with ether (3×20 mL). It was washed with brine and dried over Na_2SO_4 to give a colorless

oil without further purification (390 mg, 99%). ^1H NMR (300 MHz, $\text{DMSO}-d_6$) δ 7.52 (d, $J = 8.1$ Hz, 2 H), 7.35 (d, $J = 8.1$ Hz, 2 H), 2.93 (sept, $J = 6.9$ Hz, 1 H), 1.20 (d, $J = 6.9$ Hz, 6 H). ^{13}C NMR (75 MHz, $\text{DMSO}-d_6$) δ 162.9, 162.5, 162.1, 151.4, 136.4, 127.7,

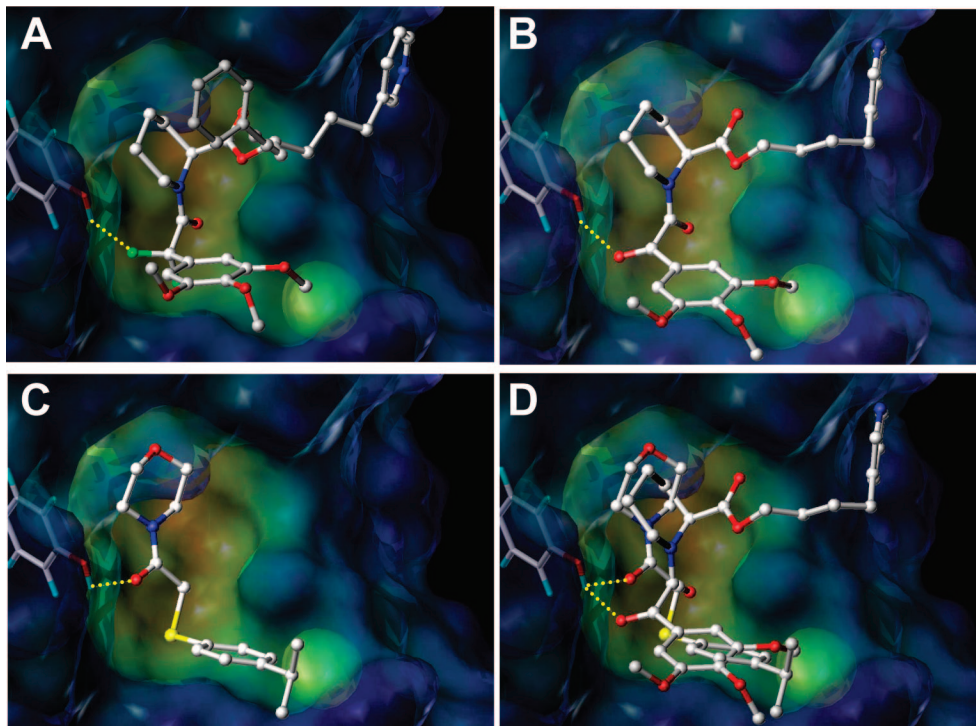


Figure 5. Molecular docking studies. (A) Surface representation of the X-ray structure of FKBP12 in complex with a previously derived inhibitor (PDB ID 1J4R).¹⁷ (B) Docked structure of a previously reported derivative of **1**.²⁵ (C) Docked structure of **6**. (D) Overlay of the docked structures shown in B and C. In all figures, hydrogen-bonding interactions between the critical Tyr26 and each compound are highlighted by a dashed line.

124.3, 121.2, 120.5, 116.7, 33.2, 23.6. HRMS m/z calcd for $C_{11}H_{11}F_2O_2S [M - H]^+$, 245.0453; found, 245.0457.

Methyl 4-(2,2-Difluoro-2-(4-isopropylphenylthio)acetyl)morpholine-3-carboxylate (8). Triethylamine (500 mg, 5.0 mmol), EDC (384 mg, 2.0 mmol), and HOBt (306 mg, 2.0 mmol) was added to a solution of 2,2-difluoro-2-(4-isopropylphenylthio)acetic acid (390 mg, 1.60 mmol) in DMF (5.0 mL) under N_2 . After the reaction mixture was stirred at rt for 30 min, methyl morpholine-3-carboxylate (295 mg, 1.63 mmol) was added. After the reaction mixture was stirred at rt for 12 h, DMF was removed under reduced pressure. It was purified by silica gel flash chromatography (EtOAc–hexanes = 1:7) to give a colorless oil (120 mg, 20%). 1H NMR (300 MHz, DMSO- d_6) δ 7.62–7.52 (m, 2 H), 7.40–7.34 (m, 2 H), 4.93 (s, 1 H), 4.32–4.22 (m, 1 H), 4.06–3.96 (m, 1 H), 3.92–3.80 (m, 1 H), 3.74 (s, 1 H), 3.72–3.64 (m, 1 H), 3.52–3.02 (m, 2 H), 3.02–2.88 (m, 2 H), 3.00–2.89 (m, 1 H), 1.24–1.08 (m, 6 H). ^{13}C NMR (75 MHz, DMSO- d_6) δ 168.9, 160.4, 151.6, 136.8, 127.7, 120.7, 66.9, 65.3, 53.2, 52.8, 43.9, 33.2, 23.6. HRMS m/z calcd for $C_{17}H_{22}F_2NO_4S [M + H]^+$, 374.1232; found, 374.1237.

Methyl 4-(2-(4-Isopropylphenylsulfonyl)acetyl)morpholine-3-carboxylate; Compound 16 (BI-69A9). 3-Chloroperoxybenzoic acid (*m*CPBA, 245 mg, 70%, 1.0 mmol) was added in small portions to a solution of methyl 4-(2-(4-isopropylphenylthio)acetyl)morpholine-3-carboxylate (**10**, 100 mg, 0.30 mmol) in CH_2Cl_2 (10 mL). After the solution had been stirred at rt for 72 h, it was washed with an excess of cold Na_2SO_3 and Na_2CO_3 solution to remove remaining *m*CPBA. It was washed with brine and dried over Na_2SO_4 . Solvent was removed under reduced pressure and the residue was purified by silica gel flash chromatography (EtOAc–hexanes = 1:4) to give a colorless oil (80 mg, 72%). 1H NMR (300 MHz, $CDCl_3$; a mixture of rotamers) δ 7.88–7.78 (m, 2 H), 4.98 (m, 1 H), 4.50–4.14 (m, 3 H), 3.96–3.82 (m, 2 H), 3.75 (s, 3 H), 3.70–3.40 (m, 3 H), 2.98 (sept, $J = 6.6$ Hz, 1 H), 1.253 (d, $J = 6.6$ Hz, 6 H). ^{13}C NMR (75 MHz, $CDCl_3$) δ 169.2, 161.7, 156.1, 136.0, 128.6, 127.5, 67.6, 66.5, 59.6, 52.9, 52.8, 44.7, 34.3, 23.6. HRMS m/z calcd for $C_{17}H_{24}NO_6S [M + H]^+$, 370.1319; found, 370.1328.

3-(3-(4-(2-(4-Isopropylphenylsulfonyl)acetyl)morpholine-3-carboxyloxy)propyl)pyridine 1-Oxide; Compound 17 (BI-69A10).

3-Chloroperoxybenzoic acid (*m*CPBA, 245 mg, 70%, 1.0 mmol) was added in small portions to a solution of 3-(pyridin-3-yl)propyl 4-(2-(4-isopropylphenylthio)acetyl)morpholine-3-carboxylate (110 mg, 0.25 mmol) in CH_2Cl_2 (25 mL). After the solution had been stirred at rt for 72 h, it was washed with excess of cold Na_2SO_3 and Na_2CO_3 solution to remove remaining *m*CPBA. It was washed with brine and dried over Na_2SO_4 . Solvent was removed under reduced pressure and the residue was purified by silica gel flash chromatography (EtOAc–hexanes = 1:1) to give a colorless oil (40 mg, 32%). 1H NMR (300 MHz, $CDCl_3$; a mixture of rotamers) δ 8.18–8.04 (m, 2 H), 7.88–7.78 (m, 2 H), 7.50–7.36 (m, 2 H), 7.24–7.16 (m, 1 H), 7.15–7.08 (m, 1 H), 4.50–4.12 (m, 5 H), 4.00–3.78 (m, 2 H), 3.74–3.44 (m, 3 H), 3.16–2.92 (m, 1 H), 2.72–2.60 (m, 2 H), 2.10–1.92 (m, 2 H), 1.27 (d, $J = 6.9$ Hz, 6 H). ^{13}C NMR (75 MHz, $CDCl_3$) δ 168.7, 161.8, 156.3, 140.2, 139.2, 137.4, 136.2, 128.6, 127.6, 126.7, 125.8, 67.7, 66.5, 64.4, 59.7, 53.1, 44.8, 34.4, 29.3, 29.1, 23.7. HRMS m/z calcd for $C_{24}H_{31}N_2O_7S [M + H]^+$, 491.1846; found, 491.1842.

2-(4-Isopropylphenylthio)-1-morpholinoethanone (6). To a solution of 2-(4-isopropylphenylthio)acetic acid (**13**; 210 mg, 1.0 mmol) in DMF (20.0 mL) was added EDC (228 mg, 1.2 mmol), HOBt (184 mg, 1.2 mmol), NEt_3 (300 mg, 3.0 mmol), and morpholine (174 mg, 2.0 mmol). After the reaction mixture was stirred at rt for 72 h, DMF was removed under reduced pressure. It was purified by silica gel flash chromatography (EtOAc–hexanes = 1:7) to give a colorless oil (100 mg, 36%). 1H NMR (300 MHz, $CDCl_3$) δ 7.39 (d, $J = 8.4$ Hz, 2 H), 7.17 (d, $J = 8.1$ Hz, 2 H), 3.69 (s, 2 H), 3.66–3.56 (m, 6 H), 1.48–3.42 (m, 2 H), 2.87 (sept, $J = 6.9$ Hz, 1 H), 1.22 (d, $J = 6.9$ Hz, 6 H). ^{13}C NMR (75 MHz, $CDCl_3$) δ 167.5, 148.6, 131.4, 127.4, 66.9, 66.6, 46.9, 42.4, 37.0, 33.8, 24.0. HRMS m/z calcd for $C_{15}H_{22}NO_2S [M + H]^+$, 280.1366; found, 280.1361.

2,2-Difluoro-2-(4-isopropylphenylthio)-1-morpholinoethanone (7). To a solution of 2,2-difluoro-2-(4-isopropylphenylthio)acetic acid (**15**; 120 mg, 0.50 mmol) in CH_2Cl_2 (10.0 mL) was added EDC (144 mg, 0.75 mmol), HOBt (114.8 mg, 0.75 mmol), NEt_3 (150 mg, 1.5 mmol), and morpholine (87.2 mg, 1.0 mmol). After the solution was stirred at rt for 24 h, the solution was washed

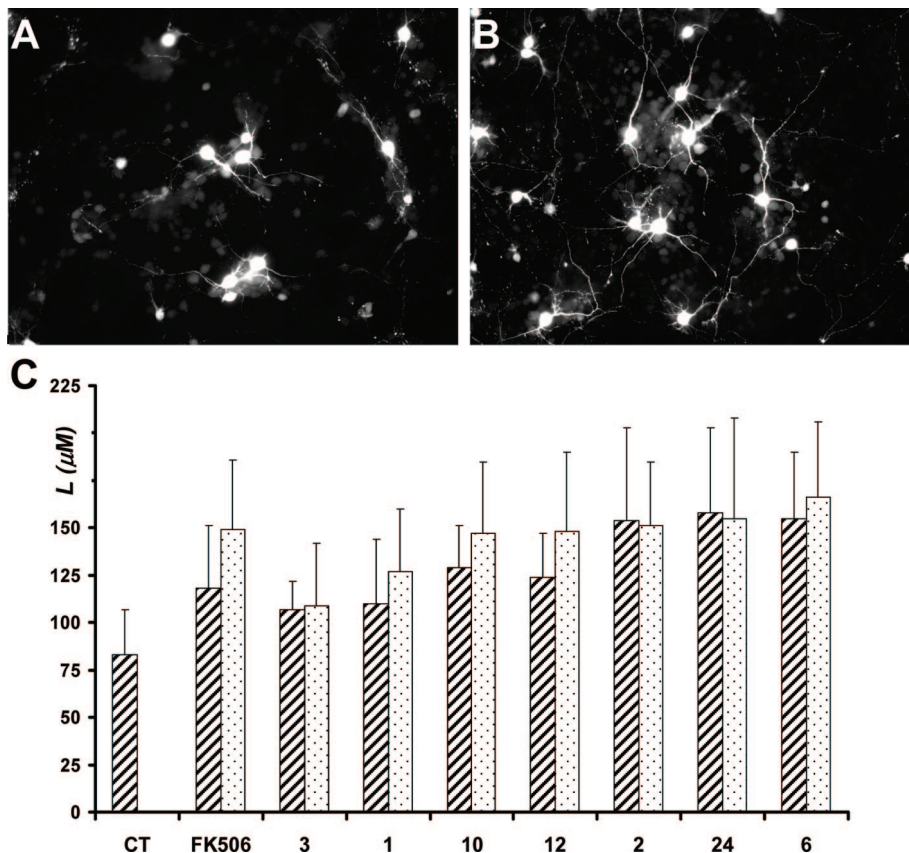


Figure 6. Compound-mediated augmentation of neurite outgrowth in cultured primary cortical rat embryonic cells. Freshly explanted cortical cells expressing transfected green fluorescent protein (GFP) were treated with (A) vehicle or (B) 1 μM **6** for 72 h. (C) The average neurite length (L) in microns was calculated from at least 10 neurons per indicated treatment (0.1 and 1 μM , for left and right bars, respectively).

with saturated NH_4Cl solution, water, saturated NaHCO_3 solution, and brine. It was dried over Na_2SO_4 , and the solvent was removed. It was purified by silica gel flash chromatography (CH_2Cl_2 , 100%) to give as a colorless oil (80 mg, 51%). ^1H NMR (300 MHz, CDCl_3) δ 7.54 (d, $J = 8.1$ Hz, 2 H), 7.26 (d, $J = 8.1$ Hz, 2 H), 3.80–3.64 (m, 8 H), 2.93 (sept, $J = 6.9$ Hz, 1 H), 1.26 (d, $J = 6.9$ Hz, 6 H). ^{13}C NMR (75 MHz, CDCl_3) δ 160.1, 151.7, 137.0, 127.5, 123.8, 121.8, 120.0, 66.8, 47.0, 43.8, 34.1, 23.0. HRMS m/z calcd for $\text{C}_{15}\text{H}_{20}\text{F}_2\text{NO}_2\text{S} [\text{M} + \text{H}]^+$, 316.1177; found, 316.1177.

3-(4-Isopropylphenyl)-1-morpholinopropan-1-one; Compound 18 (BI-69B10). To a solution of 3-(4-isopropylphenyl)propanoic acid (192 mg, 1.0 mmol) in CH_2Cl_2 (10.0 mL) was added oxalyl chloride (381 mg, 3.0 mmol) at 0 $^\circ\text{C}$. DMF (0.5 drop) was added and the solution was stirred at rt for 3 h. The solvent was removed and was coevaporated with CH_2Cl_2 (5 mL) three times. It was dissolved in CH_2Cl_2 (10.0 mL) and cooled to 0 $^\circ\text{C}$. Morpholine (100 mg, 1.2 mmol) and NEt_3 (200 mg, 2.0 mmol) was added dropwise. After it was stirred at rt for 3 h, it was washed with water (10.0 mL) and dried over Na_2SO_4 , and the solvent was removed. It was purified by silica gel flash chromatography ($\text{EtOAc}-\text{CH}_2\text{Cl}_2 = 1:3$) to give a white solid (200 mg, 77%). ^1H NMR (300 MHz, CDCl_3) δ 7.14 (d, 4 H), 3.61 (s, 4 H), 3.48 (t, $J = 4.2$ Hz, 2 H), 3.34 (t, $J = 4.5$ Hz, 2 H), 2.94 (t, $J = 7.5$ Hz, 2 H), 2.87 (sept, $J = 6.6$ Hz, 1 H), 2.60 (t, $J = 7.5$ Hz, 2 H), 1.23 (d, $J = 6.9$ Hz, 6 H). ^{13}C NMR (75 MHz, CDCl_3) δ 171.1, 147.0, 138.4, 128.5, 126.6, 66.9, 66.5, 46.1, 42.0, 35.0, 33.8, 31.2, 24.1. HRMS m/z calcd for $\text{C}_{16}\text{H}_{24}\text{NO}_2 [\text{M} + \text{H}]^+$, 262.1801; found, 262.1805.

Molecular Modeling. Docking studies were performed with GOLD version 3.0 (Cambridge Crystallographic Data Centre, Cambridge, U.K.)^{34,35} and analyzed with Sybyl (Tripos, St. Louis, MO). Molecular surfaces were generated with MOLCAD.³⁶ The X-ray coordinates of FKBP12 PDB-ID 1J4R were used to dock the compounds. Molecular models were generated with CON-

CORD³⁷ and energy-minimized with Sybyl. For each compound, 10 solutions were generated and subsequently ranked according to Chemscore (Cambridge Crystallographic Data Centre, Cambridge, U.K.).^{34,35} Top solutions were used to represent the docked geometry of the compounds and compared with the X-ray coordinates of compounds previously reported.

Human Liver Microsomal Stability. Solvents, reagents, and chemicals were purchased from VWR (San Diego, CA) in the highest grade commercially available. Human liver microsomes were purchased from BD Gentest (Boston, MA). Testosterone and 6-hydroxy testosterone and the reagents of the NADPH-generating system were purchased from Sigma (Milwaukee, WI). A mixture of the NADPH-generating system consisting of 50 μL of 2.5 mM DETAPAC, 40 μL of 5 mM NADP^+ , 40 μL of 5 mM glucose-6-phosphate, and 60 μL of glucose-6-phosphate dehydrogenase (50 IU/mL) per sample was prepared. Each incubation received 280 μL of 50 mM potassium phosphate buffer (pH 7.4) and 40 μL of a 20 mg/mL solution of pooled human liver microsomes (BD Gentest, Boston, MA). Each assay was initiated by the addition of 20 μL of a 5 mM stock of the test compound. The FK506 stock was at 0.5 mM. Aliquots were removed at 0, 10, 25, 40, and 60 min. The assay aliquots were extracted with dichloromethane/isopropanol (3:1). The tubes were centrifuged for 5 min at 4000 rpm to separate the organic and aqueous layers. The organic layer was decanted and concentrated under a stream of argon, and the residue was reconstituted with 200 μL of methanol and analyzed by RP-HPLC using a gradient of water with 0.02% perchloric acid going to 100% acetonitrile over 12 min at a flow rate of 1.5 mL/min at 254 nm.

Testosterone 6-Hydroxylase Inhibition. A mixture of the NADPH-generating system described above was prepared and 90 μL was placed into each incubation. Each incubation then received 140 μL of 50 mM potassium phosphate buffer (pH 7.4). Each incubation received 20 or 30 μL of the microsomes preparation

followed by addition of the test compound. The assay was initiated by the addition of 4 μL of a 1.45 mg/mL testosterone substrate stock to incubations, giving a final volume of 250 μL . The incubations were shaken for 10 min at 37 °C. Each incubation was terminated at 10 min by the addition of 1 mL of cold ethyl acetate. Sodium carbonate (20 mg) was added to each incubation, followed by mixing, and the mixture was centrifuged for 5 min at 4000 rpm to separate the organic and aqueous layers. The organic layer was decanted and concentrated under a stream of argon and reconstituted with 200 μL of methanol. The mixture was analyzed by RP-HPLC with a HS Supelco column at 254 nm, employing an isocratic mobile phase of water/MeOH/MeCN/HClO₄ (30:60:10:0.02, v:v) at 1 mL/min. Under these conditions, testosterone had a retention time of 6.8 min and 6-hydroxy testosterone eluted at 4.0 min.

Acknowledgment. This work was supported in part by the NIH Grants U54H9003916, XO1MH078942, and R01HL082574 (to M.P.). We thank Dr. Andrey Bobkov (BIMR) for technical assistance. We thank Dr. Anirvan Ghosh (UCSD) for his generosity with primary cortical cells and use of his laboratory facilities.

Supporting Information Available: Tables S1 and S2 report the SAR data relative to two other hits reported in Figure 2. Figure S3 consists of ¹H and ¹³C NMR spectra for synthesized FKBP12 ligands. This material is available free of charge via the Internet at <http://pubs.acs.org>.

References

- Kay, J. E. Structure–function relationships in the FK506-binding protein (FKBP) family of peptidylpropyl *cis*–*trans* isomerases. *Biochem. J.* **1996**, *314* (2), 361.
- Harrar, Y.; Bellini, C.; Faure, J.-D. FKBP12: At the crossroads of folding and transduction. *Trends Plant Sci.* **2001**, *6* (9), 426.
- Steiner, J. P.; Hamilton, G. S.; Ross, D. T.; Valentine, H. L.; Guo, H.; Connolly, M. A.; Liang, S.; Ramsey, C.; Li, J. H.; Huang, W.; Howorth, P.; Soni, R.; Fuller, M.; Sauer, H.; Nowotnik, A. C.; Suzdak, P. D. Neurotrophic immunophilin ligands stimulate structural and functional recovery in neurodegenerative animal models. *Proc. Natl. Acad. Sci. U.S.A.* **1997**, *94* (5), 2019–2024.
- Gold, B. G.; Katoh, K.; Storm-Dickerson, T. The immunosuppressant FK506 increases the rate of axonal regeneration in rat sciatic nerve. *J. Neurosci.* **1995**, *15* (11), 7509–16.
- Lyons, W. E.; George, E. B.; Dawson, T. M.; Steiner, J. P.; Snyder, S. H. Immunosuppressant FK506 promotes neurite outgrowth in cultures of PC12 cells and sensory ganglia. *Proc. Natl. Acad. Sci. U.S.A.* **1994**, *91* (8), 3191–3195.
- Sharkey, J.; Butcher, S. P. Immunophilins mediate the neuroprotective effects of FK506 in focal cerebral ischaemia. *Nature* **1994**, *371* (6495), 336–339.
- Caffrey, M. V.; Cladingboel, D. E.; Cooper, M. E.; Donald, D. K.; Furber, M.; Harden, D. N.; Harrison, R. P.; Stocks, M. J.; Teague, S. J. Synthesis and evaluation of dual domain macrocyclic FKBP12 ligands. *Bioorg. Med. Chem. Lett.* **1994**, *4* (21), 2507–2510.
- Hauske, J. R.; Dorft, P.; Julin, S.; DiBrino, J.; Spencer, R.; Williams, R. Design and synthesis of novel FKBP inhibitors. *Med. Chem.* **1993**, *35*, 4248–4296.
- Holt, D. A.; Konialian-Beck, A. L.; Hye-Ja-Oh; Yen, K.-K.; Rozamus, L. W.; Kroga, A. J.; Erhard, K. F.; Ortiz, E.; Levy, M. A.; Brandt, M.; Bossard, M. J.; Luengo, J. I. Structure–activity studies of synthetic FKBP ligands as peptidyl–propyl isomerase inhibitors. *Bioorg. Med. Chem. Lett.* **1994**, *4* (2), 315–320.
- Holt, D. A.; Luengo, J. I.; Yamashita, D. S.; Hye-Ja-Oh; Konialian-Beck, A. L.; Yen, H.-K.; Rozamus, L. W.; Brandt, M.; Bossard, M. J.; Levy, M. A.; Eggleston, D. S.; Liang, J.; Shultz, L. W.; Stout, T. J.; Clardy, J. Design, synthesis, and kinetic evaluation of high-affinity FKBP ligands and the X-ray crystal structures of their complexes with FKBP12. *J. Am. Chem. Soc.* **1993**, *115*, 9925–9938.
- Stocks, M. J.; Birkinshaw, T. N.; Teague, S. J. The contribution to binding of the pyranoside substituents in the excised binding domain of FK-506. *Bioorg. Med. Chem. Lett.* **1994**, *4* (12), 1457–1460.
- Teague, S. J.; Cooper, M. E.; Donald, D. K.; Furber, M. Synthesis and study on nonmacrocyclic FK506 derivative. *Bioorg. Med. Chem. Lett.* **1994**, *4* (13), 1581–1584.
- Teague, S. J.; Stocks, M. J. The affinity of the excised binding domain of FK-506 for the immunophilin FKBP12. *Bioorg. Med. Chem. Lett.* **1993**, *3* (10), 1947–1950.
- Wang, G. T.; Lane, B.; Fesik, S. W.; Petros, W.; Luly, J.; Krafft, G. A. Synthesis and FKBP binding of small molecule mimics of tricarboxyl region of FK506. *Bioorg. Med. Chem. Lett.* **1994**, *4* (9), 1161–1166.
- Yamashita, D. S.; Hye-Ja-Oh; Yen, S.-K.; Bossard, M. J.; Brandt, M.; Levy, M. A.; Newman-Tarr, T.; Badger, A.; Luengo, J. I.; Holt, D. A. Design, synthesis, and evaluation of dual domain FKBP ligands. *Bioorg. Med. Chem. Lett.* **1994**, *4* (2), 325–328.
- Snyder, S. H.; Sabatini, D. M. Immunophilins and the nervous system. *Nat. Med.* **1995**, *1* (1), 32–37.
- Dubowchik, G. M.; Vrudhula, V. M.; Dasgupta, B.; Ditta, J.; Chen, T.; Sheriff, S.; Sipman, K.; Witmer, M.; Tredup, J.; Vyas, D. M.; Verdoorn, T. A.; Bollini, S.; Vinitsky, A. 2-Aryl-2-difluoroacetamide FKBP12 ligands: Synthesis and X-ray structural studies. *Org. Lett.* **2001**, *3* (25), 3987–3990.
- Schreiber, S. L. Chemistry and biology of the immunophilins and their immunosuppressive ligands. *Science* **1991**, *251* (4991), 283.
- Wu, Y. Q.; Wilkinson, D. E.; Limburg, D.; Li, J. H.; Sauer, H.; Ross, D.; Liang, S.; Spicer, D.; Valentine, H.; Fuller, M.; Guo, H.; Howorth, P.; Soni, R.; Chen, Y.; Steiner, J. P.; Hamilton, G. S. Synthesis of ketone analogues of prolyl and pipecolyl ester FKBP12 ligands. *J. Med. Chem.* **2002**, *45* (16), 3558–3568.
- Armistead, D. M.; Badia, M. C.; Deininger, D. D.; Duffy, J. P.; Saunders, J. O.; Tung, R. D.; Thomson, J. A.; DeCenzo, M. T.; Futer, O.; Livingston, D. J.; Murcko, M. A.; Yamashita, M. M.; Navia, M. A. Design, synthesis, and structure of non-macrocyclic inhibitors of FKBP12, the major binding protein for the immunosuppressant FK506. *Acta Crystallogr., Sect. D* **1995**, *51* (Pt 4), 522–528.
- Xiao, H.; Wang, L. L.; Shu, C. L.; Yu, M.; Li, S.; Shen, B. F.; Li, Y. Establishment of a cell model based on FKBP12 dimerization for screening of FK506-like neurotrophic small molecular compounds. *J. Biomol. Screening* **2006**, *11* (3), 225–235.
- Hajduk, P. J.; Greer, J. A decade of fragment-based drug design: Strategic advances and lessons learned. *Nat. Rev. Drug Discovery* **2007**, *6* (3), 211–219.
- Pellecchia, M. Solution nuclear magnetic resonance spectroscopy techniques for probing intermolecular interactions. *Chem. Biol.* **2005**, *12* (9), 961–971.
- Pellecchia, M.; Becattini, B.; Crowell, K. J.; Fattorusso, R.; Forino, M.; Fragai, M.; Jung, D.; Mustelin, T.; Tautz, L. NMR-based techniques in the hit identification and optimisation processes. *Expert Opin. Ther. Targets* **2004**, *8* (6), 597–611.
- Shuker, S. B.; Hajduk, P. J.; Meadows, R. P.; Fesik, S. W. Discovering high-affinity ligands for proteins: SAR by NMR. *Science* **1996**, *274* (5292), 1531–1534.
- Hajduk, P. J.; Augeri, D. J.; Mack, J.; Mendoza, R.; Yang, J.; Betz, S. F.; Fesik, S. W. NMR-based screening of proteins containing ¹³C-labeled methyl groups. *J. Am. Chem. Soc.* **2000**, *122*, 7898–7904.
- Pellecchia, M.; Meininger, D.; Dong, Q.; Chang, E.; Jack, R.; Sem, D. S. NMR-based structural characterization of large protein–ligand interactions. *J. Biomol. NMR* **2002**, *22* (2), 165–173.
- Hamilton, G. S.; Steiner, J. P. Immunophilins: Beyond immunosuppression. *J. Med. Chem.* **1998**, *41* (26), 5119–5143.
- Wang, X. J.; Eitzkorn, F. A. Peptidyl–prolyl isomerase inhibitors. *Biopolymers* **2006**, *84* (2), 125–146.
- Yaffe, M. B.; Schutkowski, M.; Shen, M.; Zhou, X. Z.; Stukenberg, P. T.; Rahfeld, J. U.; Xu, J.; Kuang, J.; Kirschner, M. W.; Fischer, G.; Cantley, L. C.; Lu, K. P. Sequence-specific and phosphorylation-dependent proline isomerization: A potential mitotic regulatory mechanism. *Science* **1997**, *278* (5345), 1957–1960.
- Zhou, X. Z.; Lu, P. J.; Wulf, G.; Lu, K. P. Phosphorylation-dependent prolyl isomerization: A novel signaling regulatory mechanism. *Cell. Mol. Life Sci.* **1999**, *56* (9–10), 788–806.
- Goddard, T. D.; Kneller, D. G. *SPARKY 3*; University of CA, San Francisco, 2007.
- Threadgill, R.; Bobb, K.; Ghosh, A. Regulation of dendritic growth and remodeling by Rho, Rac, and Cdc42. *Neuron* **1997**, *19* (3), 625–634.
- Jones, G.; Willett, P.; Glen, R. C. Molecular recognition of receptor sites using a genetic algorithm with a description of desolvation. *J. Mol. Biol.* **1995**, *245* (1), 43–53.
- Jones, G.; Willett, P.; Glen, R. C.; Leach, A. R.; Taylor, R. Development and validation of a genetic algorithm for flexible docking. *J. Mol. Biol.* **1997**, *267* (3), 727–748.
- Teschner, M.; Henn, C.; Vollhardt, H.; Reiling, S.; Brickmann, J. Texture mapping: A new tool for molecular graphics. *J. Mol. Graph.* **1994**, *12* (2), 98–105.
- Pearlman, R. S. *CONCORD*; Tripos: St. Louis, MO, 1998.